

Nanocrystalline Microstructure and Defects in Al Solid Solution Subjected to Surface Mechanical Attrition Treatment

J. Hui¹, X. Wu^{1,2}, N. Tao³, Y. Hong², J. Lu⁴, K. Lu³

¹ Chemical Eng Dept, SH455, Cleveland State University, 2121 Euclid Avenue, Cleveland, OH44115

² State Key Lab of Nonlinear Mechanics, Institute of Mechanics, Chinese Academy of Sciences, Beijing 100080, PR China

³ Shenyang National Laboratory for Materials Sciences, Institute of Metal Research, Chinese Academy of Sciences, Shenyang 110016, PR China

⁴ LASMIS, University of Technical of Troyes, 10000, Troyes, France

Keywords: Nanocrystalline Microstructure, Dynamic Recrystallization, Surface Mechanical Attrition Treatment

Abstract

The nanocrystalline (nc) microstructure was studied in a surface layer of an Al alloy induced by the surface mechanical attrition treatment. nc grains with the larger-end of the nanometer size regime (~50-100 nm) formed through continuous refinement *via* grain subdivision mechanism, in a sequence of deformation bands with elongated subgrains, submicro-, and nc-grains leveling off ~46 nm. Meanwhile, nc grains with the lower-end of the nanometer size regime (~<10 nm) were observed to occur at a critical strain. A dynamic recrystallization mechanism was suggested to account for their formation.

1. Introduction

Nanocrystalline (nc) materials processed by severe plastic deformation are receiving ever-growing attention because of their unusual microstructure and physical and mechanical properties compared with conventional coarse-grained counterparts [1,2]. The surface mechanical attrition treatment (SMAT) is capable of synthesizing nc surface layer of the bulk material and thus producing unusual surface-related mechanical properties [3-6]. During the SAMT, microstructures of various grain size regimes, i.e. from nano-sized grains to submicro-sized and micro-sized crystallites, can be obtained within the treated surface layer along the depth from the treated surface to the strain-free matrix. This gradient structure results from a gradient change in applied strain and strain rate along the depth, from very large (top surface layer) to zero (strain-free matrix) [3]. Therefore, the SMAT offers the particular advantage of being able to study the microstructural evolution at different levels of strain and strain rate to reveal the underlying mechanism for grain refinement down to the nanometer regime. In the present study, we have investigated the microstructures and defects in the nc surface layer of an aluminum solid solution subjected to the SAMT.

2. Experimental Procedure

The material used in this investigation was an Al alloy with the chemical composition (in wt%) of 6.2 Cu, 0.5 Mn, balance Al. Prior to the SMAT of the sample, the solution heat treatment was conducted to

obtain a single solid solution phase with homogeneous coarse grains of 30 μm . The samples were in the form of 100 mm diameter and 10 mm thickness.

The SMAT method [3] was used to produce the nc surface layer. The principle of the treatment is the generation of plastic deformation on the top surface layer of a bulk material by means of repeated multidirectional impacts of flying balls (with mirror-like surface and a diameter of 7.8 mm) on the surface layer. Because of the high vibration frequency of the system (45 Hz in the present investigation), the sample surface under treatment was struck repetitively by a large number of balls within a short period of time, resulting in the sample surface becoming severely plastically deformed. The sample was protected by a high purity argon atmosphere to avoid oxidation during the SMAT at the room temperature for 15 min.

Microstructural characterization was performed using JEOL-2000FX transmission electron microscope (TEM) and JEM-2010FEF high resolution TEM for general and lattice image observations respectively. Cross-sectional thin films were prepared by means of usual sandwich method.

3. Experimental Results

3.1 nc Grains via Continuous Refinement

Figs.1 (a)-(c) are a set of cross-sectional TEM images showing the successive microstructural evolution along depth with increasing strain (corresponding to ~ 69 , 40 and 5 μm deep from the top surface respectively). Fig. 1(a) shows lamellar deformation bands characterized by elongated subgrains. The electron diffraction pattern (EDP) is typical for a subgrain structure with weak misorientations between neighboring volumes. The absorption of dislocations into the subboundary, which may lead to increase in subboundary misorientation, is frequently observed (bottom-left inset). With increasing strain, equiaxed, submicro-sized (0.1-0.4 μm) grains are present within the subsurface, as shown in Fig. 1(b). Inset is a ring-like EDP giving an evidence for creation of high boundary misorientations. A dominant feature is the formation of subgrains in plastically deformed grains of various size regimes, as shown in bottom-left inset. With further increasing strain, the grain sizes decrease down to the nanometer regime (< 100 nm) within the outer surface of the layer (from ~ 27 μm deep to the top surface). Fig. 1(c) exhibits equiaxed nc grains with the average grain size ~ 52 nm. According to the EDP, nc grains have high angle grain boundaries and random crystallographic orientations. Some grain boundaries are poorly defined and the contrast within the grain is not uniform, but often changes in a complex fashion that indicates a high level of internal stresses and elastic distortions in the crystal lattice due to the presence of a high density of dislocations at the boundaries [1]. The grain size of nc grains is observed to level off around 46 nm from ~ 10 μm deep to the top surface. X-ray diffraction analysis indicates that no other phases but FCC Al phase are detected in the SMATED surface.

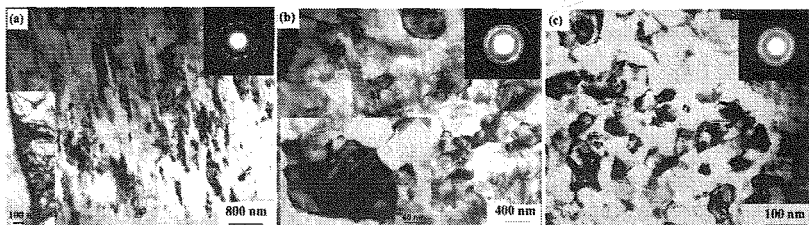


Fig. 1 Cross-sectional TEM images with EDP showing microstructural evolution with increasing strain. (a)-(c) correspond to ~ 69 , 40, and 5 μm deep from the top treated surface respectively. (a) deformation bands of elongated subgrains. Bottom-left inset exhibits absorption of dislocations into the subboundary. (b) equiaxed, submicro-sized grains. Top-right inset shows subgrains in a deformed grain. and (c) nc grains.

3.2 nc Grains with the Lower End of The Nanoscale Regime

Fig. 2 (a) is a dark-field image of nc grains obtained from the partial (111) and (200) diffraction rings (circled) of the EDP ($\sim 52\mu\text{m}$ deep). Therefore, nc grains are Al crystals. They have the lower-end of the nanometer size regime (~ 10 nm in size) as compared with those of large sizes in Fig. 1(c). Fig. 2(b) is an HREM image showing four nc grains. The fringe spacing is measured to be ~ 2 Å, which matches well with the (111) interplanar spacing of the FCC Al crystal. Detailed HREM investigations indicate that the onset of nc grains of small sizes starts to occur at a critical strain ($\sim 57\mu\text{m}$ deep), which is much low compared with that for nc grains of large sizes derived from grain refinement ($\sim 27\mu\text{m}$ deep). nc grains of small sizes are observed to form continuously and to increase their population with increasing strain.

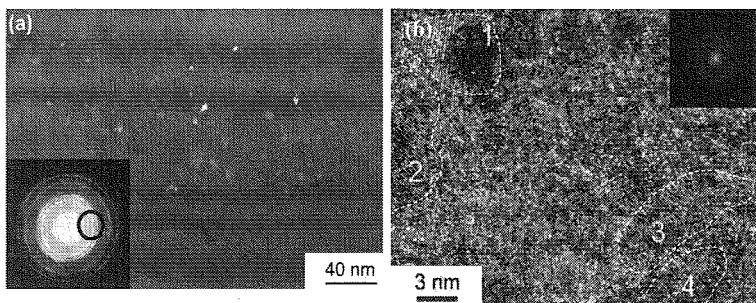


Fig. 2 (a) Dark-field TEM image showing nc grains. Inset is the EDP; (b) HREM image showing nc grains of high misorientation.

3.3 Dislocation Density

Fig. 3(a) is a Fourier reconstructed image showing one-dimensional $[-11-1]$ lattice fringes taken near the grain boundary (GB) (~ 20 nm away from the GB) of an nc grain of ~ 100 nm in diameter. Inset is the EDP with $[011]$ zone axis. Dislocations (a few are circled) are visible from the extra half planes of crystal lattices. The dislocation density is measured to be as high as $11 \times 10^{12} \text{ cm}^{-2}$, using the number of dislocations divided by the area of the figure. The dislocation density on other (11-1) and (-200) planes

are also measured to be $\sim 8.9 \times 10^{12}$ and $\sim 0.48 \times 10^{12} \text{ cm}^{-2}$ respectively. The total dislocation density within this local area is thus around $20 \times 10^{12} \text{ cm}^{-2}$. Extensive measurements are made to investigate the change in dislocation density with grain sizes and the result is shown in Fig. 3(b). Each data point represents the average from ~ 10 measurements in 3-5 grains. It is seen that the dislocation density decreases as the grain size reduces and that the dislocation density near the GBs is 1-2 order of the magnitude higher than that in grains.

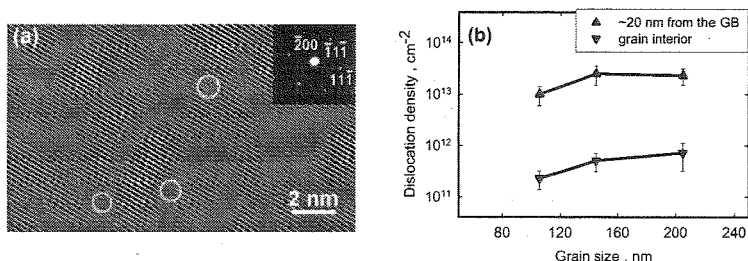


Fig. 3 (a) Fourier reconstructed image indicating high density dislocations (a few are circled). (b) dislocation density vs grain size.

Fig. 4(a) is a HREM image showing a group of nearly parallel areas (dashed line marks) where the lattice fringes are at best ill-defined or totally disappearing. When a large number of dislocations are present, they tend to form the more complicated configurations to reduce the elastic energy resulting from their mutual interactions. We therefore, prefer to call them dislocation complexes, probably due to severe strain and high strain rate during the SMAT. The disappearance of lattice fringes indicates the existence of extremely high dislocation density and intense strains. Their boundaries are rather wavy, which implies interaction with dislocations at their boundaries during deformation. It is worthwhile to note that dislocation complexes subdivide the original grain into small subgrains with dislocation complexes being their subboundaries. Moreover, equiaxed subgrains of several nanometers in size appear by intersection of multi-directional dislocation complexes (Fig. 4(b)). HREM observations further reveal that the larger the strain, the more will be the population of dislocation complexes.

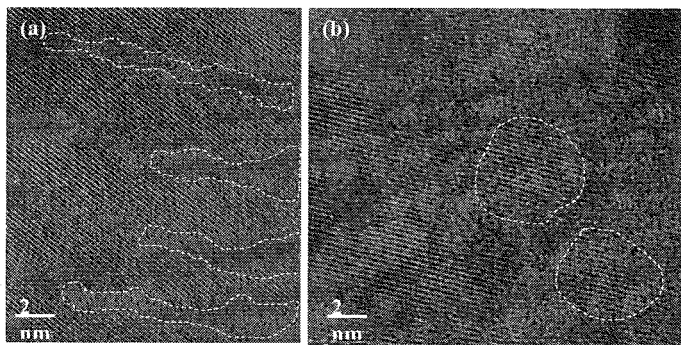


Fig. 4 HREM images showing dislocation complexes (marked dashed lines) (a) and resultant subgrains (b).

4. Discussion

TEM observations (Fig. 1) exhibit a microstructural evolution from well inside to the top surface, in a sequence of i) deformation bands with elongated subgrains, ii) equiaxed, submicro-sized grains, and iii) nc grains leveling off ~ 46 nm. The nc grains are observed to derive from continuous refinement of grains, due to the increment of strain over the whole deformed layer. The grain refinement is resulted from dislocation activity, which dominates still within the larger end of the nanometer size regime (~ 50 - 100 nm) [5-7]. Note that dislocations of high density are always present in deformed grains. As a result, the mechanism responsible for accommodating large amounts of plastic straining is to subdivide original grains into subgrains with dislocations being their boundaries [8,9], as indicated in Fig.1. With increasing strain, the microscopic grain subdivision will take place on a finer and finer scale. Simultaneously, with further increasing strain, the orientations of subgrains with respect to their neighbors become completely random and highly misoriented grain boundaries form. The increment of misorientations between neighboring subgrains may be realized by accumulating and annihilating more dislocations in subboundaries, or alternatively, by rotation of subgrains (or grain boundary sliding) with each other under certain strain [5,6]. The SAMT offers the multi-directional strain path and high strain rate, which are especially effective at promoting subgrain rotation. The present result is in good agreement with a lot of work devoted to large strain deformation [2,10].

nc grains of small sizes (Fig. 2) have the lower-end of the nanometer size regime and high misorientations. They begin to form at a critical strain, which is much low compared with that for nc grains of large sizes. They increase their population with increasing strain. Therefore, it is reasonable that nc grains are probably formed through dynamic recrystallization (DRX) triggered at a critical strain. The areas with high density dislocations will promote recrystallization nucleation as traditional materials do. It is envisaged that at these levels of dislocation density (Fig. 3), small energy fluctuations resulting from impacts during dynamic deformation process can trigger a recrystallization event. With the generation of high density dislocations and dislocation complexes, subgrains of the stored energy high enough provide favored sites for the recrystallization nucleation. The subboundary tends to be more misoriented due to accumulated rotation, which is the primary mechanism for further strain accommodation. Finally, recrystallized nc grains appear with high misorientation. The critical nucleus radius is only a few nanometers for recrystallized nc grains [11]. In the present investigation, DRX occurs at a critical strain and then operates simultaneously with grain subdivision during deformation. Such a case is very similar to the formation of nc grains *via* DRX during cryomilling Zn powders [11].

5. Summary

A nanostructured surface layer was synthesized on an Al solid solution by means of the SMAT. The crystal defects and microstructures were investigated to elucidate the mechanisms of the formation of nc grains. nc grains with the larger end of the nanometer size regime (~ 50 - 100 nm) were present *via* grain refinement operated by subdivision mechanism during deformation. nc grains with the lower end of the nanometer size regime ($\sim <10$ nm) were formed through dynamic recrystallization, which occurred at a critical strain and operated simultaneously with grain subdivision during deformation.

References

1. R.Z. Valiev, R.K. Islamgaliev, and I.V. Alexandrov, "Bulk Nanostructured Materials from Severe Plastic Deformation," *Prog. Mater. Sci.*, 45 (2000) 103-189.
2. Zhu YT et al., *Ultrafine grained materials* (Warrendale (PA): The Minerals, Metals and Materials Society, 2002).
3. K. Lu, J. Lu, J. Mater. "Nanostructured Surface Layer on Metallic Materials Induced by Surface Mechanical Attrition," *Sci. Eng., A* (2003) inprint.
4. W.P. Tong, N.R. Tao, Z.B. Wang, K. Lu, J. Lu, J., "Nitriding Iron at Lower Temperatures," *Science*, 299 (2003) 686-88.
5. N.R. Tao, Z.B. Wang, W.P. Tong, M.L. Sui, K. Lu, J. Lu, J., "An Investigation of Surface Nnanocrystallization Mechanism in Fe Induced by Surface Mechanical Attrition Treatment," *Acta mater.*, 50 (2002) 4603-4616.
6. X. Wu, N. Tao, Y. Hong, B. Xu, J. Lu, K. Lu, "Microstructure and Evolution of Mechanically-Induced Ultrafine Grain in Surface Layer of AL-Alloy Subjected to USSP," *Acta mater.*, 50 (2002) 2075-2084.
7. C. Suryanarayana, C.C. Koch, "Nanocrystalline Materials - Current Research and Future Directions," *Hyperfine Interactions*, 130 (2000) 5-44.
8. D.A. Hughes, Q. Liu, D.C. Chrzan, N. Hansen, "Scaling of Microstructural Parameters: Misorientations of Deformation Induced Boundaries," *Acta mater.*, 45 (1997) 105-112.
9. D.A. Hughes, N. Hansen, "High angle boundaries formed by grain subdivision mechanisms," *Acta mater.*, 45 (1997) 3871.
10. Y. Iwahashi, Z. Horita, M. Nemoto and T. G. Langdon. "An investigation of Microstructural Evolution during Equal-Channel Angular Pressing," *Acta mater.*, 45 (1997) 4733-4741.
11. X. Zhang, H. Wang, J. Narayan, and C. C. Koch, "Evidence for the Formation Mechanism of Nanoscale Microstructures in Cryomilled Zn Powder," *Acta mater.*, 49 (2001), 1319-1326.